Catal Lett (2010) 137:180–189
DOI 10.1007/s10562-010-0352-x

Selective Oxidation of Cyclohexane by Oxygen in a Solvent-Free System over Lanthanide-Containing AlPO-5

Jun Li · Xu Li · Yong Shi · Dongsen Mao · Guanzhong Lu

Received: 3 February 2010 / Accepted: 14 April 2010 / Published online: 30 April 2010
© Springer Science+Business Media, LLC 2010

Abstract Ln-containing AlPO-5 (Ln = La, Ce, Sm, Dy, Y, Gd) were synthesized hydrothermally in the presence of HF, and characterized by XRD, UV-vis, SEM, N_2 adsorption/desorption, FT-IR, solid state ^{27}Al MAS NMR and ICP-AES techniques. The results showed that all the samples had good crystallinity and high specific area. Isomorphous substitution of Ln ions for Al^{+3} occurred. The lanthanide ions were incorporated into the frameworks or were highly dispersed on extra frameworks of the samples. The newly synthesized catalysts all were efficient for the oxidation of cyclohexane in a solvent-free system, especially Gd–AlPO-5. Near 13% conversion of cyclohexane were achieved on the catalyst Gd(60)–AlPO-5 with Al/Gd of 60 under the conditions of 0.5 MPa O_2, 413 K and 4 h reaction. The total selectivity to cyclohexanol and cyclohexanone was up to 92%. In addition, the catalyst Gd(60)–AlPO-5 was recyclable for the titled reaction system.

J. Li (✉) · X. Li · Y. Shi · D. Mao · G. Lu
Research Institute of Applied Catalysis, Shanghai Institute of Technology, 200235 Shanghai, People's Republic of China
e-mail: junliecust0967@sina.com

X. Li
e-mail: 1987xuli@163.com

Y. Shi
e-mail: shiyong@sit.edu.cn

D. Mao
e-mail: dsmao1106@yahoo.com.cn

G. Lu
e-mail: gzhlu@ecust.edu.cn

G. Lu
Research Institute of Industrial Catalysis, East China University of Science and Technology, 200235 Shanghai, People's Republic of China

Keywords Cyclohexane · Oxidation · Lanthanide · AlPO-5

1 Introduction

Heterogeneous catalytic oxidations are of growing importance for modern chemical industry, such as selective oxidation of cyclohexane. Cyclohexane can be oxidized to cyclohexanol and cyclohexanone, which are important intermediates in the production of adipic acid and caprolactam. Caprolactam is often used to manufacture nylon-6 and nylon-66 polymers [1–4]. In addition, cyclohexanol and cyclohexanone were also used as the solvent of lacquers and homogenizers for soaps and synthetic detergent emulsions [2]. However, cyclohexane oxidation was considered to be the least efficient in all major industrial chemical processes [5]. Cyclohexane conversion was lower than 5% in order to obtain high selectivity to the goal products. Moreover, in most cases, extreme reaction conditions such as high pressure and high temperature in conjunction with low activity make the process less attractive. So, it's necessary to find environmentally friendly catalytic system for activation of cyclohexane under mild reaction conditions.

Recently, some new catalyst materials and catalytic systems have been developed for the selective oxidation of cyclohexane. Fe(III) and Mn(III) complexes were synthesized and employed as catalysts in the oxidation of cyclohexane under mild conditions, conversion up to 10.2% (4.2 and 6.0 yields for cyclohexanol and cyclohexanone, respectively) was obtained [6]. However, these processes were carried out in acetonile. The reaction systems with hydrogen peroxide as oxidant and acetic acid as solvent could achieve selective oxidation of cyclohexane

under moderate conditions, but the problem of the leaching of transition metal should be solved [7, 8]. Recently, three-dimensional mesoporous materials Cr- and Co-TUD-1 were reported to be active in the oxidation of cyclohexane with tert-butylhydroperoxide (TBHP), and above 90% selectivity towards mono oxygenated products was achieved at conversion levels as high as 8–10% [9]. Good results were also obtained while mesoporous materials such as Ti-MCM-41 [10], V-MCM-41 [11], Bi-MCM-41 [12] and V-MCM-48 [13] were used as catalysts for the oxidation of cyclohexane, but organic solvents were usually added and TBHP or hydrogen peroxide were applied as the oxidant, which may resulted in the contamination of the products and environmental problems [14]. Fe-MCM-41 was tested as catalyst for the selective oxidation of cyclohexane, and excellent results were obtained [15]. Unfortunately, acetic acid was used as a solvent, and initiator (methyl ethyl ketone) must be used. Selective photocatalytic-oxidation of cyclohexane was studied, and very high selectivity to cyclohexanone was obtained [16]. Photocatalytic oxidation of cyclohexane was a promising method [17], but the reaction rate needs to be improved greatly. Reference [18] presented a good review on heterogeneous catalysts for hydrocarbon oxidation and many details about this work can be found therein.

Molecular oxygen is the cheapest and cleanest oxidant with the highest content of active oxygen species. Effective use of molecular oxygen for selective oxidation of cyclohexane is a topic of great interest. In addition, the solvent plays an important role in most processes of catalytic cyclohexane oxidation, This may lead to many environmental problems. However, activation of cyclohexane by molecular oxygen in a solvent-free system is still a challenge although a few systems have been reported [2].

Cobalt porphyrin was used as catalyst in solvent-free systems [19]. The results indicated that the catalyst was very efficient, but cobalt porphyrin is too expensive. Au/ZSM-5 [20], and Au/MCM-41 [21] were found to be very efficient, but the leaching of gold nanoparticles from the carrier was quite serious. Bi/MCM-41 was also found to be an efficient catalyst for the selective oxidation of cyclohexane [12], but the price of bismuth is very high, which prevent the application of Bi/MCM-41 on a large scale. Hybrid materials formed by the combination of chromium-containing inorganic compounds and organotrialkoxysilanes were reported to possess good activity towards selective oxidation of cyclohexane in solvent-free systems [22].

$AlPO_4$-n molecular sieves have a much more flexible framework compared with zeolites, and allow the substitution of Al^{3+} and/or P^{5+} by transition metal ions. One of the important promising applications of AlPO-n is the aerial oxidations of linear and cyclic hydrocarbons [23, 24]. They are also available in the growing field of solvent-free industrial reactions in the important area of clean technology. Interesting catalytic properties may be created by the substitution processes. Substitution of Al^{3+} and/or P^{5+} by one type of transition metal ions was extensively studied [25, 26]. The channel geometry of MnAlPO4–5 affords facilities for the diffusion of cyclohexane, which led to higher turnover rates on MnAlPO4–5 than on MnAlPO4–18 with small channels [24]. Recently, incorporation of two different transition metal ions in the framework of AlPO4–5 were studied by Fan and co-workers, important and interesting information was obtained [8]. The kinetics and mechanism of cyclohexane oxidation were studied in details [24, 27], which will be very helpful for well understanding the reaction.

Owing to their unique catalytic activities associated with environmental concerns, CeO_2 and CeO_2-based materials, such as CeO_2–SiO_2, CeO_2–TiO_2 and CeO_2–ZrO_2 [28], have been widely investigated. A general conclusion is that solid solutions formed by incorporation of MO_x into the lattice of CeO_2 possess higher oxygen storage capacity and better redox properties than those of CeO_2 alone. Our group have synthesized a cerium doped AlPO-5, and investigated the catalytic performance of the new material by the selective oxidation of cyclohexane. Results showed that Ce–AlPO-5 was an efficient catalyst [2]. Encouraged by the previous work, we have studied lanthanide-doping AlPO-5 molecular sieves in order to find more efficient catalysts for the oxidation of cyclohexane.

Here, we have shown a series of lanthanide-doping AlPO-5 molecular sieves. Detailed characterization of these materials was carried out by numerous physical–chemical methods. The materials were studied as catalysts for the oxidation of cyclohexane with O_2 as an oxidant. Out of the synthesized catalysts, Gd(60)-AlPO4–5 was found to be the best for the selective oxidation of cyclohexane.

2 Experiment

2.1 Synthesis of Catalysts Ln–AlPO-5

The chemical reagents used in the present study were of AR grade. The Ln–AlPO-5 samples (Ln = La, Ce, Sm, Dy, Y, Gd) were synthesized according to references [2] with minor modifications, in which HF acid was used. The preparation procedure is as follows: A calculated amount of phosphoric acid (85 wt%), triethylamine (TEA), and one type of the lanthanide metal ion nitrate and deionized water were mixed together at 30 °C and stirred for 2 h, then aluminium isopropylate was added to this mixture under stirring. After the slurry was further stirred for 2 h at 30 °C, HF (40% in water) diluted with water was added

under stirring, and this mixture was stirred continually for another 2 h. The molar compositions of the matrix gels are: $xLn(NO_3)_3{\cdot}6H_2O{:}Al_2{\cdot}O_3{:}1.3P_2O_5{:}1.6TEA{:}1.3HF{:}425H_2O$. The molar ratios of Al/Ln are 100, and the corresponding products are expressed as Ln–AlPO-5, while the molar ratios of Al/Gd for other Gd-doped AlPO-5 are 20, 40, 60 and 80, the relevant products are expressed as Gd(20)–AlPO-5, Gd(40)–AlPO-5, Gd(60)–AlPO-5 and Gd(80)–AlPO-5, respectively. The matrix gel were finally transferred into a Teflon-lined stainless steel autoclave, and crystallized at 180 °C for 24 h without stirring. After the autoclave was quenched in cold water, the product was separated by centrifugation, washed with de-ionized water repeatedly, dried at 100 °C for 20 h and calcined in air at 550 °C for 5 h. The contents of the lanthanide in the synthesized catalysts were analyzed by ICP-AES and the results are shown in Table 1.

2.2 Characterization of the Samples

The chemical–physical properties of the prepared samples were analyzed by Powder XRD, N_2 adsorption/desorption, scanning electron microscopy (SEM), FT-IR, UV-Vis DRs, ^{27}Al MAS NMR spectra and ICP-AES.

XRD patterns were recorded with a RigakuD/MAX 2550 PC diffractometer equipped with Ni-filtered Cu Kα radiation (scanning step 0.15° s^{-1}). BET surface areas and pore diameter distribution of the samples were measured according to the N_2 adsorption isotherms measured by a Micrometrics ASAP 2010. Fourier transform infrared (FT-IR) spectroscopy was obtained on an AVATAR 360 FT-IR spectrometer for a resolution of 4 cm^{-1} in KBr media at room temperature. The diffuse reflectance (DR) UV-vis spectra were recorded on a Varian Cary 100 spectrometer with an integration sphere in the region 800–200 nm at split width of 1.5 nm and a scan speed of 400 nm min^{-1}, in which the baseline was corrected by using a calibrated sample of barium sulfate. The chemical compositions of the matrix gels and the calcinated samples were determined by inductively coupled plasma-atomic emission spectroscopy (Scan 16, TJA Corporation). Solid state ^{27}Al MAS-NMR measurements were performed using Bruke AVANCE III 500 NMR spectrometer at 130.3 MHz and a rotation rate of 5 kHz. Approximately 3000 scans were accumulated. Solid state ^{27}Al chemical shifts were reported relative to 1.0 M $Al(NO_3)_3$ aqueous solution.

2.3 Oxidation of Cyclohexane with Molecular Oxygen

The catalytic oxidation was carried out in a 25 mL stainless steel reactor equipped with a magnetic stirrer. In a typical reaction, cyclohexane (2 mL) was mixed with one of the prepared catalysts (10 mg) and then heated to the reaction temperature. After that, oxygen was charged into the reactor to 0.5 MPa. During the course of the reaction, the stirring speed was about 320 rpm. When the reaction was completed, the mixture of the reactant and products was cooled down and centrifuged to separate the catalyst. The products were identified by GC-MS (Agilent 6890 N/5973 N). Excess triphenylphosphine was added to the mixture in order to convert cyclohexyl hydroperoxide to cyclohexanol [29]. Cyclohexanone and cyclohexanol were analyzed quantitatively on a GC9790 (Wenling Corp. Ld., Shanghai China) gas chromatograph equipped with an capillary column (30 m long, 0.32 mm i.d., 0.25 μm film thickness) and a FID detector using toluene as the internal standard. The conversion was calculated based on the starting cyclohexane. Owing to their decomposition in the condition of the chromatograph analysis, cyclohexyl hydroperoxide and organic acids (probably including

Table 1 Elemental compositions and structure characteristics of the synthesized catalysts

Sample	Al/Ln (mol) of the matrix gel	2θ (°)	d_{100} (Å)	Ln content (wt%) of the formed products	BET surface area (m^2 g^{-1})	BJH adsorption cumulative volume of pores (cm^3 g^{-1})
AlPO-5	∞	7.5	11.8	0	239	0.33
Ce-AlPO-5	100	7.3	12.0	0.89	289	0.39
Sm-AlPO-5	100	7.3	12.0	0.95	289	0.39
Dy-AlPO-5	100	7.4	11.9	1.03	279	0.37
Y-AlPO-5	100	7.4	12.0	0.57	270	0.35
La-AlPO-5	100	7.3	12.0	0.88	288	0.38
Gd-AlPO-5	100	7.4	12.0	1.0	279	0.37
Gd(80)-AlPO-5	80	7.3	12.0	1.23	287	0.36
Gd(60)-AlPO-5	60	7.3	12.0	1.61	289	0.40
Gd(40)-AlPO-5	40	7.3	12.0	2.35	262	0.35
Gd(20)-AlPO-5	20	7.4	12.0	4.54	264	0.35

d_{100}: XRD (100) interplanar spacing

succinic acid, glutaric acid, valeric acid, caproic acid and adipic acid) could not be analyzed by GC exactly [1]. In this paper, cyclohexyl hydroperoxide was determined by iodometric titration and the organic acids were analyzed by GC after being converted into their respective methyl ester as described earlier [4].

Recycling tests were carried out by repeatedly using Gd(60)–AlPO-5 in five consecutive reactions under 0.5 MPa O_2 at 140 °C for 4 h. After each reaction, the catalyst was separated by filtration from the reaction solution, washed with acetone, dried at 393 K for 10 h, and reused in the next run under the same reaction conditions.

3 Results and Discussion

3.1 Catalyst Characterization

3.1.1 Powder X-Ray Diffraction

The XRD patterns in Fig. 1 show that the samples synthesized have the typical AFI structures with an extremely intense (100) line at about 7.4° and a high crystallinity. No impure crystalline phase was detected, which reveals that Ln may be highly dispersed on the extra framework or Ln atoms partially substitute aluminium atoms in the framework by forming a new Ln–AlPO structure [30]. It was found that all reflections in the XRD patterns of Ln-containing samples shifted to lower positions, as compared to the pure AlPO-5 molecular sieve. The results indicated that addition of Ln in the synthesis gel led to an enlargement of the unit-cell volume as a result of the unit-cell expansion [8], which was further confirmed by the data shown in Table 1. The shift of diffraction peaks to lower angle with an incorporation of lanthanide can be ascribed to the bigger diameter of the incorporated ions.

3.1.2 FT-IR Spectroscopy

The FT-IR absorption spectra of the synthesized catalysts, the pure AlPO-5 and The Ln–AlPO-5 samples, were shown in Fig. 2. All the samples show a characteristic absorption band at $\sim$3440 cm^{-1} that is assigned to the vibration absorption of the Al–OH groups of the synthesized samples. In the range of 400–1600 cm^{-1}, three peaks at $\sim$465, $\sim$706, and $\sim$1130 cm^{-1} are corresponding to the rocking, symmetric stretching, and asymmetric stretching of the inter-tetrahedral oxygen atoms in the AlPO-5, respectively. Compared with the pure AlPO-5, the absorption peaks of the Ln–AlPO-5 samples shift slightly toward the lower wave number, for instance, the absorption peak at $\sim$1130 cm^{-1} of AlPO-5 shifts to about 1120 cm^{-1} of Ln–AlPO-5. In general, the change of the absorption peaks

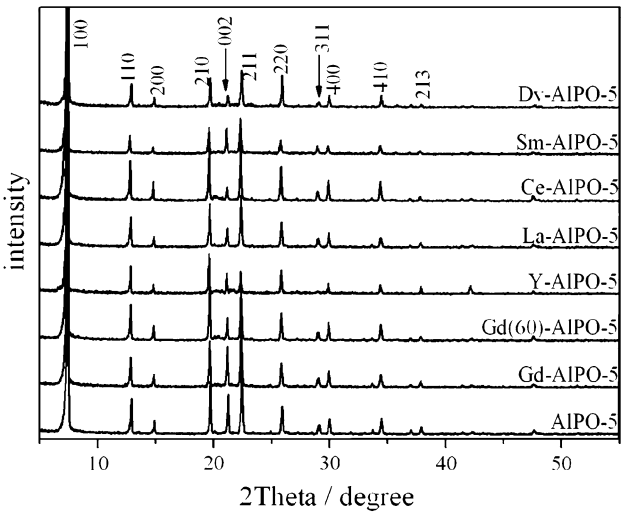

Fig. 1 XRD patterns of the samples AlPO-5, Gd(60)-AlPO-5 and Ln-AlPO-5

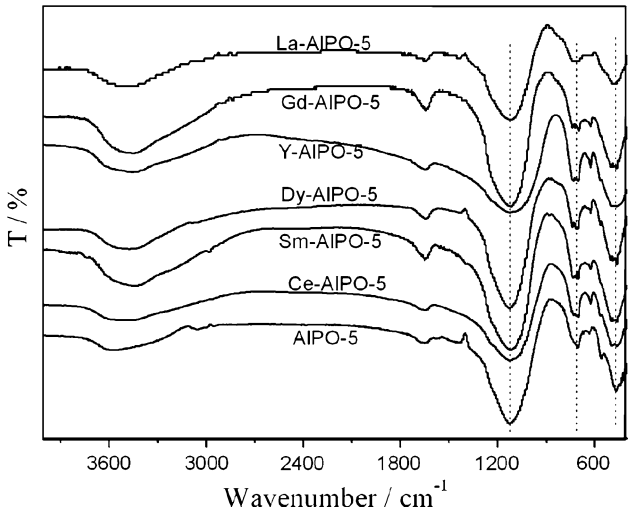

Fig. 2 FT-IR spectra of the samples AlPO-5 and Ln-AlPO-5

is indicative of Ln incorporating into the framework of AlPO-5 tetrahedral as the lengths of Ln–O bonds are longer than that of Al–O bond [31, 32].

3.1.3 Diffuse-Reflectance UV-Vis Spectroscopy

It is known that the UV-vis spectroscopy of the sample is a very sensitive probe for an identification and characterization of transition metal ion coordination and its existence in the framework and/or on the extra framework position of metal-containing zeolites [22]. UV-Vis spectra of the Ln–AlPO-5 samples are presented in Fig. 3. There are an obvious absorption peak at about 256 nm and a broad absorption band with a maximum at $\sim$300 nm for the sample Ce–AlPO-5, while only one distinct absorption peak is found for every other sample, which locates at

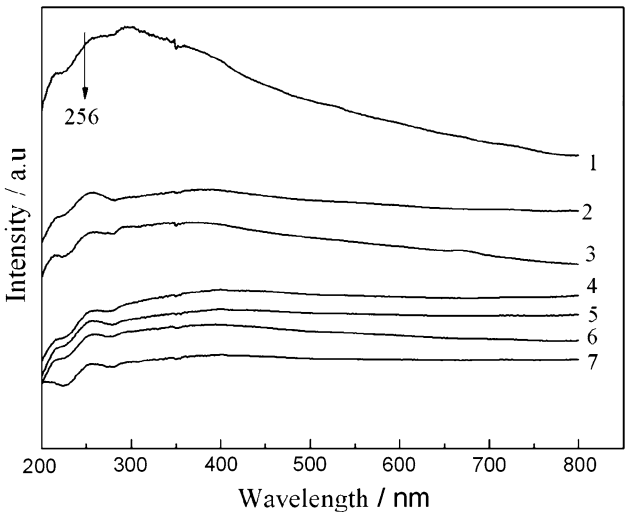

Fig. 3 UV-vis spectra: (*1*) Ce-AlPO-5, (*2*) Y-AlPO-5, (*3*) Gd(20)-AlPO-5, (*4*) Gd-AlPO-5, (*5*) Dy-AlPO-5, (*6*) La-AlPO-5, (*7*) Sm-AlPO-5

about 256 nm. The position of absorption peaks and absorption band associates with the charge transfer from ligand to metal depends on the ligand field symmetry surrounding the Ln center. The electronic transition from oxygen to Ln requires a higher energy for tetra-coordinated Ln ions than for hexa-coordinated Ln. Therefore, the absorption bands at about 256 nm are due to the charge transfer from O^{-2} to tetra-coordinated Ln(III) in the samples, whereas the adsorption peaks at higher wavelength ($\sim$300 nm) for the sample Ce–AlPO-5 may be assigned to the charge transfer from O^{-2} to hexa-coordinated Ce specie on the extra framework [33]. According to the above analysis, the Ce specie may present partly in the framework and partly dispersed highly on the extra framework of the ample Ce–AlPO-5. For the samples Gd(20)–AlPO-5 and Ln–AlPO-5 (Ln = Y, Gd, Dy, La, Sm), the rare-earth ions have been incorporated into the framework of the Ln-containing aluminophosphate molecular sieves.

3.1.4 Solid State 27Al MAS NMR Measurements

Solid state ^{27}Al MAS NMR measurements of the samples AlPO-5 and Gd–AlPO-5 were taken to provide convincing evidence for the framework incorporation of ion Gd in the newly-prepared aluminophosphate material. The solid state ^{27}Al magic-angle spinning (MAS) NMR spectra of the synthesized AlPO-5 and Gd-AlPO-5 molecular sieves were collected (Fig. 4a and b). The ^{27}Al MAS NMR spectra of the pure AlPO-5 and the Gd-containing sample all displayed two peaks. The intense signal at around 37 ppm for the AlPO-5 and the signal at around 39 for the sample Gd–AlPO-5 can be ascribed to the tetrahedral aluminium atoms in the AFI structure. The resonance peaks at about

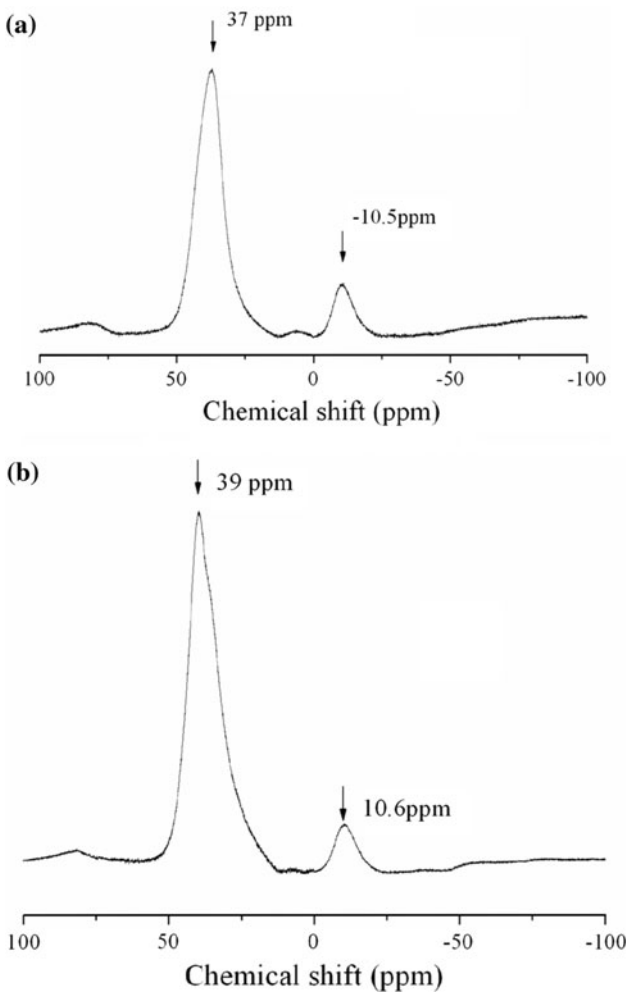

Fig. 4 ^{27}Al MAS NMR spectra of the samples (**a**) AlPO-5 and (**b**) Gd-AlPO-5

10–11 ppm are assigned to hexacoordinated Al, which are possibly formed by water adsorption. It was reported that the adsorption of water in aluminophosphate molecular sieves caused the appearance of resonance peaks in the pentacoordinated and octahedral regions in the solid state ^{27}Al MAS NMR spectrum [8, 34]. A significant shift of tetrahedrally coordinated ^{27}Al was observed when transition metal ions were incorporated in the framework of AlPO-5 [8]. As shown in the Fig. 4, the band position of the Gd–AlPO-5 is slightly different from that of the pure AlPO-5. The position of the main peak for the Gd-containing sample shifts by 2 ppm in contrast with the position of the sample AlPO-5. This can be thought as a convincing evidence for the isomorphous substitution of Gd^{+3} for Al^{3+} in the Gd–AlPO-5 sample. This is in agreement with UV-vis analysis results.

3.1.5 N_2 Adsorption/Desorption Isotherm

N_2 adsorption/desorption isotherms and pore diameter profiles of the synthesized AlPO-5 and Ln–AlPO-5

samples are shown in Fig. 5a and b, BET surface area and pore volume of the samples are presented in Table 1. For all the synthesized samples, the BET surface areas are more than 230 m^2 g^{-1}. With the incorporation of lanthanide, the pore volume somewhat increases, the specific surface areas also become bigger. Especially, the BET surface area and the pore volume both increase by about 21% for Gd(60)–-AlPO-5 compared with AlPO-5. These results clearly demonstrate that incorporation of lanthanide in the AlPO-5 sample leads to a modification of its surface texture. As shown on the isotherms, the quantity adsorbed/desorbed is a little bigger for Gd–AlPO-5 than for AlPO-5. The result may be related to the bigger pore volume of the synthesized Gd-AlPO-5. The pore diameter distribution of the as prepared materials are narrow, this indicates that the size of the structural pores is uniform. Moreover, the pore size distributions of the AlPO-5 and Gd–AlPO-5 are very similar as evidenced by the Fig. 5b

3.1.6 Surface Microstructure

Scanning electron microscopy (SEM) was used to determine the particle size and particle morphology of the synthesized sample. The SEM pictures of the Gd-doping AlPO-5 in Fig. 6a and b show the morphology of hexangular rhombic-like rods which is typical for AFI-type materials. It is clear that most of the particles are rod-like. The similar SEM images were also observed by Utchariyajit [35] and Rakoczy [3] who synthesized AlPO-5 using microwave radiation and traditional hydrothermal method, respectively.

The agglomerates or crystalline impurities presented in the previous paper [2] generally arose from water content, the molar ratio of Al to Ce in the reaction system, or the crystallization time in the Teflon-lined autoclaves, and are hardly seen in the present picture Fig. 6a. However, the details about the formation of the agglomerates need more work to be done.

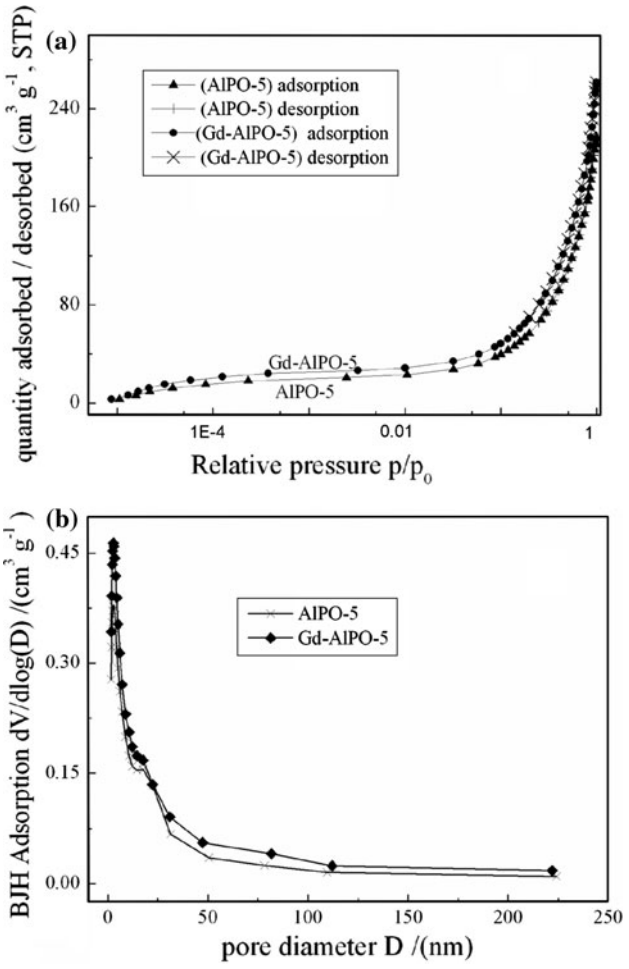

Fig. 5 **a** adsorption–desorption isotherms and **b** the pore size distribution for Gd-AlPO-5 and AlPO-5

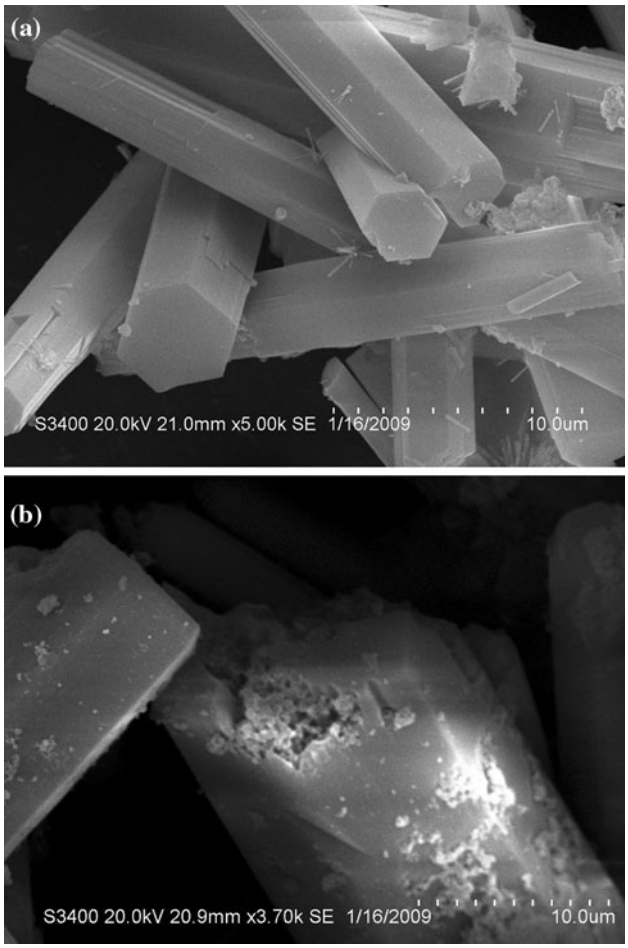

Fig. 6 SEM images of **a** Gd-AlPO-5 and **b** Gd(60)-AlPO-5

3.2 Catalytic Performance

The type, content, and valence of lanthanide ions in aluminophosphates may have a significant influence on the catalytic property of the synthesized materials, it is necessary to perform an extensive study on the catalytic performance of the Ln-containing AlPO-5. The catalytic performances of the newly-prepared materials for the oxidation of cyclohexane under the conditions of 0.5 MPa O_2 and 413 K are given in Table 2. It is shown that all samples exhibit catalytic activity with cyclohexanone and cyclohexanol as the major products. Significant amount of oxidative products were detected in the blank reaction over pure AlPO-5 although the conversion of cyclohexane was much lower than that on other catalysts. This result indicates the presence of lanthanide in AlPO-5 plays a role in the catalytic reaction.

The content of cyclohexyl hydroperoxide in the blank reaction system is much higher than that in the other systems with Ln–AlPO-5 as a catalyst. This result indicates the doped metals in AlPO-5 account for the decomposition of cyclohexyl hydroperoxide. In many earlier reports about the selective oxidation of cyclohexane to cyclohexanone with solid catalysts, tert-butylhydroperoxide (TBHP) was added into the reaction system as free-radical initiator in order to accelerate the initiation step of the auto oxidation process using molecular oxygen as oxidant [1]. The present results displayed in Table 2 reveal that the catalyst Ln–AlPO-5 is effective for the selective oxidation of cyclohexane using molecular oxygen as oxidant without extra free-radical initiator or co-catalyst.

The total selectivities of cyclohexanone, cyclohexanol and cyclohexyl hydroperoxide are high and close over Ce–AlPO-5, Sm–AlPO-5, Dy–AlPO-5, Y–AlPO-5 and Gd–AlPO-5 in contrast to that over La-AlPO-5, indicating the catalyst La–AlPO-5 is unsuitable to the selective oxidation of cyclohexane although the conversion of cyclohexane is high. Among the Ln–AlPO-5 catalysts, Gd–AlPO-5 shows the best activity for the oxidation of cyclohexane with good selectivity to the goal products, while the higher activity of Ce–AlPO-5 reported by Zhao [2] was not observed in the current research. This difference may be apparently assigned to the crystalline impurities in the material displayed in the paper [2]. Compared with other newly-prepared catalysts, Gd–AlPO-5 is the most efficient catalyst with both high conversion and selectivity for the selective oxidation of cyclohexane in the solvent-free system.

With an increase of Gd content from (Al/Gd) 100–60, the conversion of cyclohexane and the selectivity to the desired product cyclohexanone increased a little. The activity of the catalysts Gd-doped AlPO-5 decreased somewhat with further increase of Gd content after (Al/Gd) 60, while the selectivity to cyclohexanone decreased and the selectivity to cyclohexanol increased when Al/Gd was lower than 60 as shown in Fig. 7. The content of cyclohexyl hydroperoxide kept low, and no obvious changes was found for the Al/Gd from 100 to 60. The above result may be related to the structure of the synthesized materials and the dispersion of Gd in the aluminophosphate molecular sieve [36]. Some of the Gd-atoms may be in the state of conglomeration when the ratio of Al/Gd is lower than 60, this may lead to the lower activity. Figure 8 illustrates the influence of the reaction temperature. With raising reaction temperature from 130 to 160 °C, the conversion of cyclohexane increased monotonously although the increase was slight for the temperature from 140 to 160 °C. The selectivity to cyclohexanone changed somewhat, but the

Table 2 Oxidation of cyclohexane over different catalysts

Catalyst	Time (h)	Temperature (K)	Conversion (%)	Selectivity (%)					-one/-ol
				-one	-ol	CHHP	-one+(-ol)+CHHP	Others	
AlPO-5	4	413	2.0	25.3	29.6	31.2	86.1	13.9	0.9
Ce-AlPO-5	4	413	9.9	56.2	35.1	4.1	95.4	4.6	1.6
Sm-AlPO-5	4	413	9.4	50.2	38.9	3.9	93	7	1.3
Dy-AlPO-5	4	413	10.6	47.9	40.2	4.5	92.6	7.4	1.2
Y-AlPO-5	4	413	8.4	56.6	33.6	3.8	94	6	1.7
La-AlPO-5	4	413	10.1	49.1	33.9	2.9	85.9	14.1	1.4
Gd-AlPO-5	4	413	12.2	58.5	33.5	3.8	95.8	4.2	1.7
Gd-AlPO-5	4	433	13.1	57.6	28.9	1.1	87.6	12.4	2.0
Gd-AlPO-5	6	413	12.8	59.1	30.6	1.4	91.1	8.9	1.9

Reaction conditions: 2 ml cyclohexane, 10 mg catalyst, 0.5 MPa O_2, at 413 K, 4 h. Ln-AlPO-5: Al/Ln = 100(mole ratio), Ln = Ce, Sm, Dy, Y, La, Gd

CHHP cyclohexyl hydroperoxide, *-one* cyclohexanone, *-ol* cyclohexanol. Others, including mainly adipic acid and glutaric acid (about 85% of the byproducts); small amounts of succinic acid, valeraldehyde, valeric acid, caproic acid; trace of methyl cyclohexane and amyl alcohol

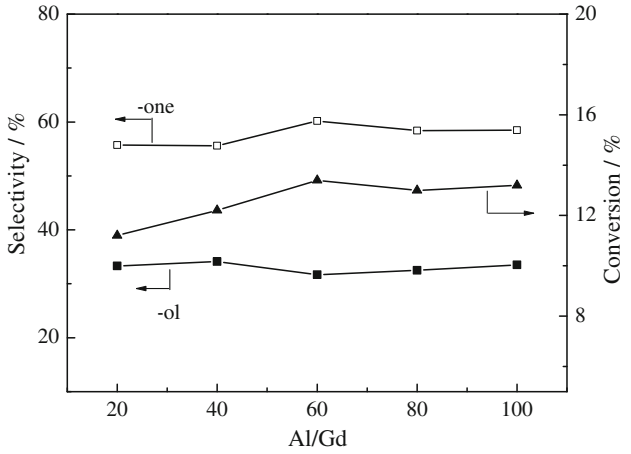

Fig. 7 Conversion of syclohexane and selectivities of CHHP, cyclohexanone (-one) and cyclohexanol (-ol) with respect to Al/Gd (reaction conditions: 2 mL cyclohexane, 10 mg Gd-doped AlPO-5 catalyst, 0.5 MPa O_2, at 413 K, 4 h)

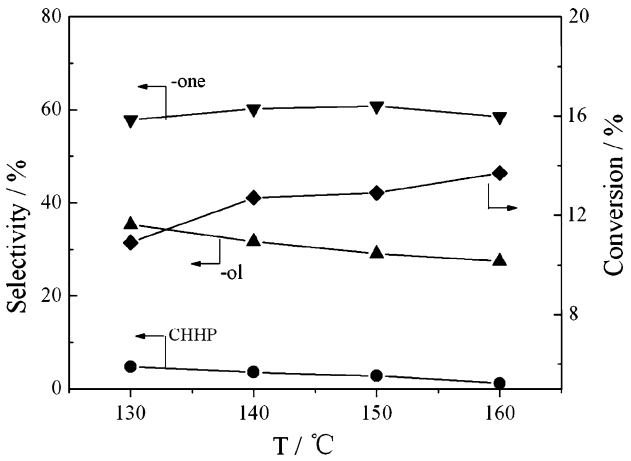

Fig. 8 Conversion of cyclohexane and selectivities of CHHP, cyclohexanone (-one) and cyclohexanol (-ol) with respect to reaction temperature (reaction conditions: 2 mL cyclohexane, 10 mg catalyst Gd(60)-AlPO-5, 0.5 MPa O_2, 4 h)

selectivity to cyclohexanol decreased obviously. Cyclohexyl hydroperoxide decreased with increase of temperature, implying that cyclohexyl hydroperoxide decomposed to other chemicals [24, 36]. The result here differs from the report in reference [22] where the conversion of cyclohexane remained was in the same level after 140 °C. The difference may be ascribed to the catalyst used. For this reason, the most proper reaction temperature was in the range of 140 to 160 °C, and thus selected as reaction temperatures for the subsequent studies.

The reaction time may have an important effect on the result. Figure 9 displays the experiment data for the effect of the time with the synthesized Gd(60)–-AlPO-5 as the catalyst. With increasing reaction time from 4 to 10 h, the

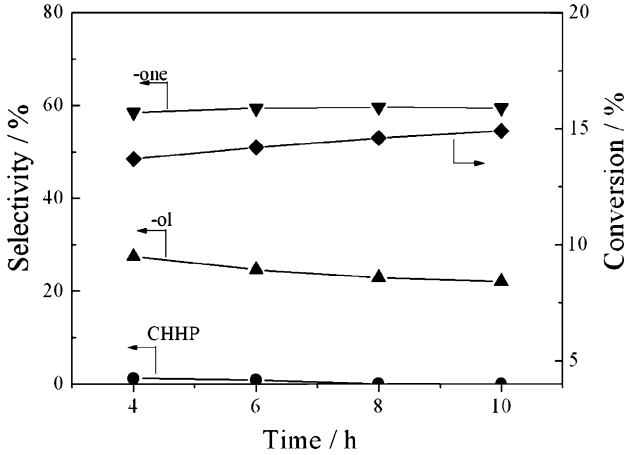

Fig. 9 Conversion of cyclohexane and selectivities of CHHP, cyclohexanone (-one) and cyclohexanol (-ol) with respect to reaction time (reaction conditions: 2 mL cyclohexane, 10 mg catalyst Gd(60)-AlPO-5, 0.5 MPa O_2, at 433 K)

conversion of cyclohexane exhibits almost a linear increase and the selectivity to cyclohexanone increases gradually, while the selectivities to cyclohexyl hydroperoxide and cyclohexanol decrease due to decomposition of cyclohexyl hydroperoxide and further oxidation of cyclohexanol to cyclohexanone [24]. These results suggest that the primary products formed are cyclohexyl hydroperoxide and cyclohexanol, as cyclohexanol is more reactive than cyclohexane [22]. In addition, extending reaction time leads to a decrease in total selectivity with a slight increase in conversion, possibly resulting from deep oxidation of cyclohexanol and cyclohexanone [24, 27].

The reaction mechanism and kinetics of cyclohexane oxidation have previously been studied [24, 27, 36, 37]. It was thought that cyclohexane reacted with O_2 on metal-containing catalysts, then cyclohexanol and cyclohexanone formed through an intermediate, Cyclohexyl hydroperoxide (CHHP). Here, the CHHP-mediated pathways can be used to analyze the kinetic results of this study. CHHP was formed on Gd(60)–AlPO-5, it parallel decomposed to cyclohexoxy radicals ($RO^{\bullet}$) and peroxyl radicals ($ROO^{\bullet}$). $RO^{\bullet}$ and $ROO^{\bullet}$ reacted with cyclohexane to produce cyclohexanol and cyclohexanone respectively. Also, $ROO^{\bullet}$ radicals may recombined to form cyclohexanol and cyclohexanone, while cyclohexanol may be oxidized to cyclohexanone. the overoxidation of cyclohexanone led to the formation of adipic acid and other byproducts.

To confirm that the catalyst is heterogeneous, Hot-filtration study was performed with the catalyst Gd(60)–AlPO-5. The leaching tests were carried out at 403 k under 0.5 MPa O_2. The catalyst was removed hot after 2 h and 4 h reactions in the two separate experiments. Then the filtrates were monitored for further reaction rates, but no increases in conversion were noted. The filtrates were also

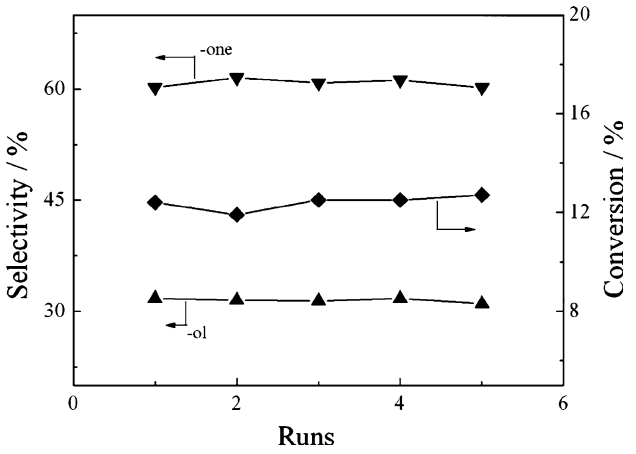

Fig. 10 Conversion of cyclohexane and selectivities of cyclohexanone (-one) and cyclohexanol (-ol) with respect to recycle times (reaction conditions: 2 mL cyclohexane, 10 mg catalyst Gd(60)-AlPO-5, 0.5 MPa O_2 at 413 K, 4 h)

analyzed by ICP-AES, No cerium was detected. These results suggest that Gd(60)-–AlPO-5 behaved as a heterogeneous catalyst, and the catalyzed reactions were truly heterogeneous.

The catalytic stability of the sample Gd(60)–AlPO-5 was further explored. Five reaction runs were carried out in the same condition. The results on the catalyst are shown in Fig. 10. It is clear that within five reaction recycles, the conversion of cyclohexane and the selectivity to both cyclohexanone and cyclohexanol change a little. No obvious difference in Gd content between the fresh and recycled catalysts was detected by ICP-AES. These results indicate that the catalyst is stable or reusable after the reaction. The stability of the synthesized catalytic material can be attributed to the distribution of gadolinium in the Gd(60)–AlPO-5, that is, most of the gadolinium entered the internal surface or framework of AlPO-5, as revealed by the above characterization.

4 Conclusions

AlPO-5 variants with the lanthanide La, Ce, Sm, Dy, Y, Gd incorporated into the framework were successfully synthesized under hydrothermal conditions in the presence of HF. The various characterization techniques proved that the metals were partially occupied the position of Al(III) and incorporated into the framework of AlPO-5. All the synthesized catalytic materials Ln–AlPO-5 were active for the oxidation of cyclohexane by oxygen in a solvent-free system, while Gd(60)–AlPO-5 was the most efficient catalyst of the newly synthesized materials with a conversion of nearly 13% and a total selectivity of about 92% to cyclohexanone and cyclohexanol under feasible conditions. Moreover, the reaction system is environmentally friendly, the catalyst Gd-doped AlPO-5 is very stable. In summary, Gd-doped AlPO-5 is a promising catalyst and deserved to be developed further.

Acknowledgments The authors acknowledge financial support from Shanghai Institute of Technology (KJ 2007-01) and the Committee of Science and Technology of Shanghai (06-JC-14095), China.

References

1. Zhou L, Xu J, Miao H, Wang F, Li X (2005) Appl Catal A: Gen 292:223–228
2. Zhao R, Wang Y, Guo Y, Guo Y, Liu X, Zhang Z, Wang Y, Zhan W, Lu G (2006) Green Chem 8:459–466
3. Hermans I, Peeters J, Jacobs PA (2008) J Phys Chem A 112:1747–1753
4. Anand R, Hamdy MS, Parton R, Maschmeyer T, Jansen JC, Hanefeld U (2009) Appl Catal A: Gen 355:78–82
5. Yao W, Fang H, Ou E, Wang J, Yan Z (2006) Catal Commun 7:387–390
6. Salomãoa Gisele C, Olsena Mara HN, Dragob V, Fernandesc C, Filhod LC, Antunes OAC (2007) Catal Commun 8:69–72
7. Silva AC, Fernández TL, Carvalho NMF, Herbst MH, Bordinhão J, Adolfo H Jr, Wardell JL, Oestreicher EG, Antunes OAC (2007) Appl Catal A: Gen 317:154–160
8. Fan W, Fan B, Song M, Chen T, Li R, Dou T, Tatsumi T, Weckhuysen BM (2006) Micro Meso Mater 94:348–357
9. Anand R, Hamdy MS, Gkourgkoulas P, Maschmeyer T, Jansen JC, Hanefeld U (2006) Catal Today 117:279–283
10. Zahedi-Niaki MH, Kapoor MP, Kaliaguine S (1998) J Catal 177:231–239
11. Selvam P, Dapurkar SE (2005) J Catal 229:64–71
12. Qian G, Ji D, Lu GM, Zhao R, Qi YX, Suo JS (2005) J Catal 232:378–386
13. Selvam P, Dapurkar SE (2004) Appl Catal A: Gen 276:257–265
14. Unnikrishnan RP, Endalkachew S-D (2002) Chem Commun 214–2147
15. Suanta K, Selvam P (2004) Chem Lett 33:198–199
16. Du P, Moulijn JA, Mul G (2006) J Catal 238:342–352
17. Kluson P, Luskova H, Cerveny L, Klisakova J, Cajthaml T (2005) J Mol Catal A: Chem 242:62–67
18. Sheldon RA, Wallau M, Arends IWCE, Schuchardt U (1998) Acc Chem Res 31:485–493
19. Guo C, Chu M, Liu Q, Liu Y, Guo D, Liu X (2003) Appl Catal A: Gen 246:303–309
20. Zhao R, Ji D, Lv G, Qian G, Yan L, Wang X, Suo J (2004) Chem Commun 904–905
21. Lü G, Zhao R, Qian G, Qi Y, Wang X, Suo J (2004) Catal Lett 97(3–4):115–118
22. Shylesh S, Samuel PP, Singh AP (2007) Appl Catal A: Gen 318:128–136
23. Thomas JM, Raja R, Sankar G, Bell RG (2001) Acc Chem Res 34:191–200
24. Modén B, Zhan BZ, Dakka J, Santiesteban JG, Iglesia E (2007) J Phys Chem C 111:1402
25. Fan W, Weckhuysen BM, Schoonheydt RA (2001) Phys Chem Chem Phys 3:3240–3246
26. Beale AM, Grandjean D, Kornatowski J, Glatzel P, Groot FM, Weckhuysen BM (2006) J Phys Chem B 110:716–722
27. Hermans I, Peeters J, Jacobs PA (2008) J. Phys Chem A 112:1747–1753

28. Reddy BM, Khan A, Lakshmanan P, Aouine M, Loridant S, Volta JC (2005) J Phys Chem B 109:3355–3363
29. Tian P, Liu ZM, Wu ZB, Xu L, He YL (2004) Catal Today 93–95:735–742
30. Larese C, Galisteo FC, Granados ML, López RM, Fierro JLG, Lambrou PS, Efstathiou AM (2004) Appl Catal B : Environ 48: 113–123
31. Goubin F, Rocquefelte X, Whangbo MH, Montardi Y, Brec R, Jobic S (2004) Chem Mater 16:662–669
32. Natile MM, Glisenti A (2005) Chem Mater 17:3403–3413
33. Zhan W, GLU GuoY, Guo Y, Wang Y (2008) J Rare Earth 26:59–65
34. Luis GH, Carlos MÁ, Furio C, Fernando LA, Joaquín PP (2008) Chem Mater 20:987–995
35. Utchariyajit K, Wongkasemjit S (2008) Micro Meso Mater 114:175–184
36. Modén B, Oliviero L, Dakka J, Santiesteban JG, Iglesia E (2004) J. Phys Chem B 108:5552–5563
37. Modén B, Zhan BZ, Dakka J, Santiesteban JG, Iglesia E (2006) J Catal 239:390–401